Article

Non-Energy Valorization of Residual Biomasses via HTC: CO$_2$ Capture onto Activated Hydrochars

Katia Gallucci * ⬤ **, Luca Taglieri, Alessandro Antonio Papa, Francesco Di Lauro, Zaheer Ahmad and Alberto Gallifuoco**

Industrial Engineering Department, University of L'Aquila, Monteluco di Roio—67100 L'Aquila, Italy; luca.taglieri@univaq.it (L.T.); alessandroantonio.papa@graduate.univaq.it (A.A.P.); francesco.dilauro@student.univaq.it (F.D.L.); zaheer.ahmad@graduate.univaq.it (Z.A.); alberto.gallifuoco@univaq.it (A.G.)

* Correspondence: katia.gallucci@univaq.it

check for updates

Abstract: This study aims to investigate the CO$_2$ sorption capacity of hydrochar, obtained via hydrothermal carbonization (HTC). Silver fir sawdust was used as a model material. The batch runs went at 200 °C and up to 120 min. The hydrochar was activated with potassium hydroxide impregnation and subsequent thermal treatment (600 °C, 1 h). CO$_2$ capture was assayed using a pressure swing adsorption (PSA) process. The morphology and porosity of hydrochar, characterized through Brunauer-Emmett-Teller, Barrett-Joyner-Halenda (BET-BJH) and scanning electron microscopy (SEM) analyses, were reported and the sorbent capacity was compared with traditional sorbents. The hydrochar recovered immediately after the warm-up of the HTC reactor had better performances. The Langmuir equilibrium isotherm fits the experimental data satisfactorily. Selectivity tests performed with a model biogas mixture indicated a possible use of hydrochar for sustainable upgrading of biogas to bio-methane. It is conceivably a new, feasible, and promising option for CO$_2$ capture with low cost, environmentally friendly materials.

Keywords: hydrochar; hydrothermal carbonization; biogas upgrading; CO$_2$ capture; pressure swing adsorption

1. Introduction

Growing population and economy race are the two main concerns regarding the increase in emissions of greenhouse gases (GHG) and, subsequently, the accelerating climate change and global warming. Carbon dioxide is the first responsible for these unwanted effects [1]. Nowadays, reducing CO$_2$ emissions is one of the most challenging issues facing humanity [2]. Global climate reports show that the average world temperature is steadily increasing with respect to 20th century data [3]. Besides, worldwide researchers recognize the need for a sustainable development and more equity, including poverty eradication, and provide an ethical foundation for limiting the effects of climate changes. The rate of atmospheric accumulation of GHGs and the capacity to address its mitigation and adaptation differ for each nation. Often, many of the countries most vulnerable to climate change contribute little to GHG emissions.

Intergovernmental panel on climate change (IPCC) recently reported on the impacts of global warming of 1.5 °C above pre-industrial levels and the related global greenhouse gas emission pathways [4]. The attention is on the decision to adopt the Paris Agreement [5,6].

Comprehensive and sustainable strategies in response to climate change should consider the co-benefits, adverse side-effects, and risks inherent to both adaptation and mitigation options. European policy options emerge in the European Union (EU) Emission Trading System (ETS) that involve the

promotion of investment on clean and low carbon technologies in power and heat generation, energy-intensive industry sectors, materials, and chemicals' production. The legislative framework of the EU Emission Trading System (ETS) achieved the EU's 2030 emission reduction targets [7] and contributed to the 2015 Paris Agreement. Now, the goals include keeping the rise in temperature below 2 °C, that is, CO_2 below 450 ppm [8].

Practical ways to meet these goals could be planting trees, caring the existing forests, rebuilding of soils, and developing the biomass-to-energy chain with coupled with carbon capture and storage.

Carbon dioxide capture/separation onto solid matrices is broadly studied for reducing greenhouse gas discharge [9]. Also, biofuels and bio-methane are strategic for fuel transition to sustainability, or as a reagent in the steam and dry reforming and catalytic processes. A paradigm is biogas production by anaerobic digestion of organic matter. The mixture mainly consists of 40 vol% to 75 vol% methane and 15 vol% to 60 vol% carbon dioxide [10,11].

Biogas cleaning and upgrading to bio-methane require to remove water, foam, dust H_2S, and trace components, as well as CO_2 [11] and bio-methane production, in Europe is spreading progressively [12]. In Italy, such technology struggles to spread with only five operating plants and a total upgrading capacity of 500 Nm^3/h. The delay is mainly owing to the imprecise legislative references regarding grid injection techniques. As a mean to overcome these limits, an effort was made toward the development of implementing rules and guidelines for accessing the incentives.

From a purely technological point of view, several techniques are available for commercial use, at laboratory and industrial scale [13–18]. CO_2 capture technologies, like absorption and adsorption, are proliferating as commonly used capture techniques worldwide, as proven by the several patent applications and published articles [19]. Adsorbent media include activated carbon, alumina, metallic oxides, and zeolites. The regeneration of the adsorbent is carried out by temperature or pressure swing adsorption (TSA or PSA) [20]. For TSA, solid adsorbents with a lower heat capacity are claimed for reducing the energy required for regeneration [21–23].

The most important property of an adsorbent is its CO_2 adsorption capacity, which depends strongly on the pore structure, the surface area, and the type of functionalization. Besides, the capacity depends on the partial pressure of CO_2, temperature, and humidity [24,25]. Absorption proved to not be economical for treating flue gas streams with CO_2 partial pressures lower than 15 vol% [26]. Chemical absorption has relatively high selectivity, but also high energy consumption for regeneration, chemicals' make-up, and high environmental impact [27,28]. Taking into account the potential role of porous carbon materials for CO_2 capture, the authors propose the production of these materials starting from renewable sources, mainly residual biomasses.

Hydrothermal carbonization (HTC) is an alternative synthesis method to produce precursors for high value-added renewable carbon materials from residual lignocellulosic biomasses [29]. This thermochemical conversion occurs in hot compressed water, at a relatively low temperature under autogenous pressure [30]. HTC optimization was studied considering the re-use of the liquid phases in the process itself [31,32], the online monitoring of the carbonization time-course [33,34], and the recovery of valuable platform chemicals from the liquid [35,36].

Hydrochar attracts the attention for several potential applications, mainly in support of the energy production chain [37,38]. Nevertheless, owing to its coal-like structure, hydrochar could be favorably transformed into porous activated carbon with tunable morphologies and porosities, which is hard to achieve using traditional pyrolytic methods, with a surface area up to 3000 m^2g^{-1} and pore volume in the range of 0.5–1.5 cm^3g^{-1} [39,40].

The focus of this paper is on the separation of CO_2 for the upgrading of biogas to bio-methane by PSA onto HTC from silver fir sawdust, a waste product available in Central Europe and *Abies* species available worldwide [41].

2. Materials and Methods

2.1. Synthesis of Carbon Porous Sorbent

2.1.1. Materials

The tested biomass was silver fir sawdust. All HTC experiments were performed using demineralized water (σ = 0.005 mS/cm). Potassium hydroxide (Sigma-Aldrich Comporation US, grade ACS reagent, Reg. Ph. Eur.) and HCl (Sigma-Aldrich grade puriss, 24.5%–26.0%) were used for the activation of the hydrochar.

2.1.2. Experimental Apparatus

The HTC apparatus was designed and realized on purpose. Details of the piping and control instrumentation are reported elsewhere [34]. The 316-stainless steel batch reactor has an internal volume of about 200 mL and is equipped with a valve for the air initial evacuation and gaseous product withdrawal. A thermocouple and a pressure-meter allow monitoring and controlling the process temperature and pressure, respectively.

2.1.3. Experimental Procedure

The HTC experiments were performed at 200 °C, with a constant water biomass ratio 7:1, and residence time equal to 0 and 120 min. The substrate was ground in a mortar and sieved. The fraction below 1 mm was recovered and used for the reaction after drying until constant weight in an oven, at 105 °C. Demineralized water and dry biomass were loaded into the reactor in the chosen weight ratio. Then, the reactor was sealed, evacuated for about 15 min, and heated up to the process temperature. The warm-up lasted for about 20–25 min. Residence time was measured once it reached the temperature set point. At the end of the run, the reactor was quenched with air until 160 °C, and then with water until room temperature.

After the quenching step, the gas phase was recovered and weighed. Solid and liquid products were recovered and separated by filtration. The filter and solid phases were put in an oven at 105 °C for at least 24 h for dry weight determination. After drying, the hydrochar was milled and sieved (certified ISO 3310–1 & 2 and ASTM E11, Endecott sieves). The fraction between 106 and 355 μm was recovered and stored in vials before the CHNS characterization (data reported in Supplementary Material) and the activation step. Then, 15 grams of 1:2 solid mixture of hydrochar and KOH was put in an oven under nitrogen gas flow and warmed up to 600 °C (3 °C/min). The dwell step lasted 1 h [40]. The samples were washed with 10 wt% HCl to remove any inorganic salts, and then with demineralized water until neutral pH. Finally, the samples were dried in an oven at 105 °C for 24 h.

2.1.4. Characterization Methods

The nitrogen sorption isotherms of activated and non-activated hydrochars were determined with a high-speed surface area and pore size analyzer NOVA 1200e Alfates Quartachrome. Brunauer-Emmett-Teller (BET) [42] and Barrett-Joyner-Halenda (BJH) [43] methods were utilized for a standard determination of surface area, pore volume, and pore size distribution and the average pore diameter [44]. Each sample was outgassed for 3 h at 100 °C.

Textural properties were investigated by means of scanning electron microscopy and energy dispersive X-ray spectroscopy (SEM-EDS). The analyses were performed with a Field Emission Zeiss Gemini500SEM analyser (acceleration voltage from 0.02 to 30 KV—store resolution up to 32 k × 24 k pixels—0.6 nm at 15 KV, in back-scattering electron mode—pressure from 5 to 500 Pa), equipped with EDS (energy dispersive spectroscopy) microanalyzer OXFORD Aztec Energy with INCA X-ACT PELTIER COOLED ADD detector. All samples were coated with 5 nm of Cr in an automatic sputter coater Q 150T ES.

2.2. CO_2 Adsorption Test

2.2.1. Materials

Three hydrochar types were tested, namely, HC_200_0 (non-activated, residence time 0 min), HCA_200_0 (activated, residence time 0 minute), and HCA_200_120 (activated, residence time 120 min). Grain size ranged from 106 μm to 355 μm. Nitrogen (grade 5.5), methane (grade 4.5), and carbon dioxide (grade 4.0) were used for dynamic adsorption tests (Rivoira Spa). Blank tests were performed, packing the column with glass beads (2500 kg/m^3, 106–355 μm).

2.2.2. Experimental Apparatus

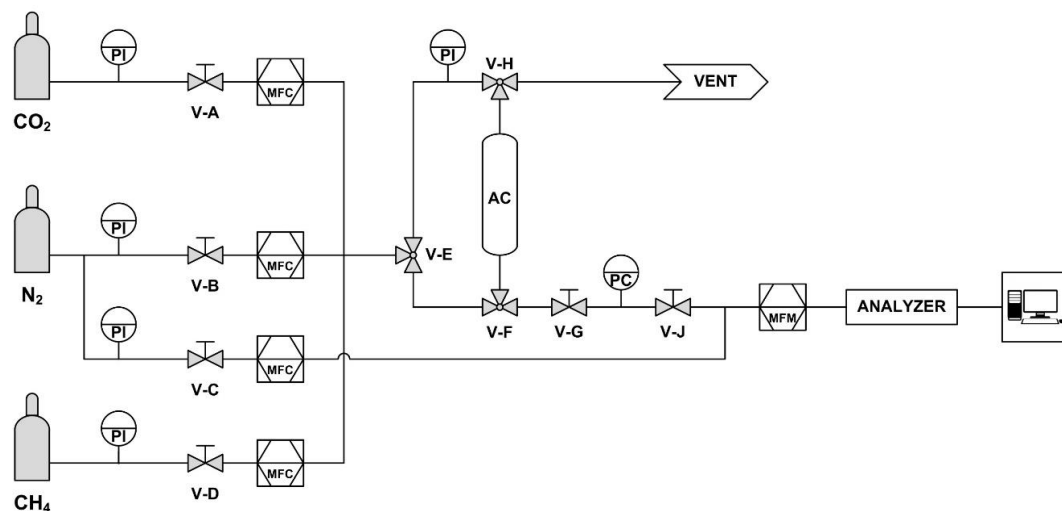The experimental apparatus is shown in Figure 1.

Figure 1. Flowsheet of the experimental apparatus: PI—pressure indicator; V-i—valves; MFC—mass flow controller; MFM—mass flow meter; PC—pressure controller; AC—adsorption column; analyzer—URAS ABB.

Details of the piping and control instrumentation are reported in a previous paper [22].

2.2.3. Experimental Procedure

Bed length was kept constant packing the column with the same HC volume same of the inert material volume used for the blank test.

Adsorption experiments were performed with two different feed mixtures (CO_2 + N_2 and CO_2 + CH_4). The PSA operating pressure varied up to 5 bars.

Tests with CO_2 + N_2 were carried out at 2, 3, 4, and 5 bar with 100 NmL/min of CO_2 and 80 NmL/min of N_2 (carrier gas). The regeneration step was performed with N_2 at 280 NmL/min. A mass flow meter (MFM) quantified the total amount of the gas mixture leaving the column. During the adsorption tests, V-A, V-B, and V-C valves were kept open. The configuration for regeneration after each run was as follows: V-A and V-G closed, V-H switched for a quick depressurization and then repositioned, V-G re-opened, and N_2 injected until no CO_2 was detected. The blank tests were carried out in the same way.

Tests with CO_2 + CH_4 mixture were carried out at 2 and 5 bar with 76 NmL/min of CO_2 and 76 NmL/min of CH_4. The flow rate of N_2 during the regeneration step was 280 NmL/min. The experiments were carried out as previously described, with CH_4 in the inlet flow rate instead of N_2. V-D and V-A operated simultaneously. The regeneration step lasted until no CH_4 was detected at the column outlet.

All tests were repeated almost five times. The synopsis is reported in Table 1.

Table 1. Synopsis of tests conditions.

Test	Hydrothermal Conditions	Adsorption Conditions		Activation
	Time [min]	P [bar]	W_{BED} [g]	
CO_2/N_2				
HC_200_120_2	120	2	1.135	no
HC_200_120_3	120	3	1.135	no
HC_200_120_4	120	4	1.135	no
HC_200_120_5	120	5	1.135	no
HCA_200_0_2	0	2	0.695	yes
HCA_200_0_3	0	3	0.695	yes
HCA_200_0_4	0	4	0.695	yes
HCA_200_0_5	0	5	0.695	yes
HCA_200_120_2	120	2	1.135	yes
HCA_200_120_3	120	3	1.135	yes
HCA_200_120_4	120	4	1.135	yes
HCA_200_120_5	120	5	1.135	yes
CO_2/CH_4				
HCA_200_0_2	0	2	0.695	yes
HCA_200_0_5	0	5	0.695	yes

2.2.4. Mathematical Model

The mathematical model for determining the amount of the adsorbed CO_2 was extensively described in Di Felice et al. [45]. The blank test highlighted the domination in the response curve of a flow-mixing in the ancillary equipment and provided a means of confronting the gas outlet responses to the CO_2 capture characteristics of the bed itself. A simple descriptive FOPDT model (first order plus dead time model) of the gas phase allows extracting the response of the particle phase from the measured gas phase response of the entire system under CO_2 capture conditions. The response curve gives the molar total gas holdup, viz, the product of the total molar throughput of gas and the area enclosed by the response curve and normalized ordinate 1 (Figures 2 and 3).

The response curve may be used to evaluate the total amount of CO_2 present in the whole system as a function of time (i.e., its holdup: the moles of CO_2 that entered the system at time t minus those that left). The CO_2 holdup in the solid phase of the bed (i.e., the CO_2 captured by the hydrochar) is merely the total holdup of the entire system minus the holdup of the gas phase of the entire system [45]. Adsorption performance in CO_2/CH_4 tests was evaluated estimating recovery, purity, and selectivity [22]. The gas recovery rate is the ratio of the quantity of gas recovered after the column to the fed quantity:

$$\text{Recovery}(i) = \left(\int_0^t (y_i\, q)_{\text{OUT}}\, dt \right) \Big/ \left(\int_0^t (y_i\, q)_{\text{BLANK}}\, dt \right) \tag{1}$$

The purity is defined by the quantity of the gas during the saturation phase divided by total gas leaving the column at the same time.

$$\text{Purity}(i) = \left(\int_0^t (y_i\, q)_{\text{OUT}}\, dt \right) \Big/ \left(\int_0^t q_{\text{OUT}}\, dt \right) \tag{2}$$

where y_i is the molar fraction of the specific gas and q is the total gas flow.

The selectivity is expressed as follows:

$$\text{Selectivity} = \frac{\text{mol}_{CO_2}/\text{kg}_{\text{adsorbent}}}{\text{mol}_{CH_4}/\text{kg}_{\text{adsorbent}}} \tag{3}$$

3. Results and Discussions

The assessment of new porous carbon material should be based on its adsorption properties, evaluated through the well-established procedures. Table 2 lists the results of the BET analysis.

Table 2. BET and BJH results of all materials tested.

Sample Parameters	Surface Area (A_{BET}) [m^2/g]	BJH Desorption Pore Volume (V_{BJH}) [cm^3/g]	Average Diameter of the Pores $(D_{av,BJH})$ [Å]
HC_200_0	1.13	0.004	142
HCA_200_0	881	0.241	11
HC_200_120	1.33	0.008	241
HCA_200_120	284	0.109	15

The surface area and the average diameter of the pore $D_{av,BJH}$ (obtained as $4 \cdot V_{BJHa}/A_{BET}$, where V_{BJHa} is the BJH desorption pore volume and A_{BET} is the BET surface area) are critical parameters for physical adsorption. In general, the higher the superficial area, the better the sorbent capacity.

The increase of porosity is also highlighted by SEM-EDS images (Figure 2), where, in the left-hand side (Figure 2a,c,e), the original wood structure is always present after hydrothermal treatment with several typical pits [46] and, at higher magnification (3000 and 10,000×), 10 μm macropores are also visible. On the right-hand side (Figure 2b,d,f), after the activation procedure, as expected, a well-developed sponge structure is evident at increasing magnification (400, 2000, and 10,000×).

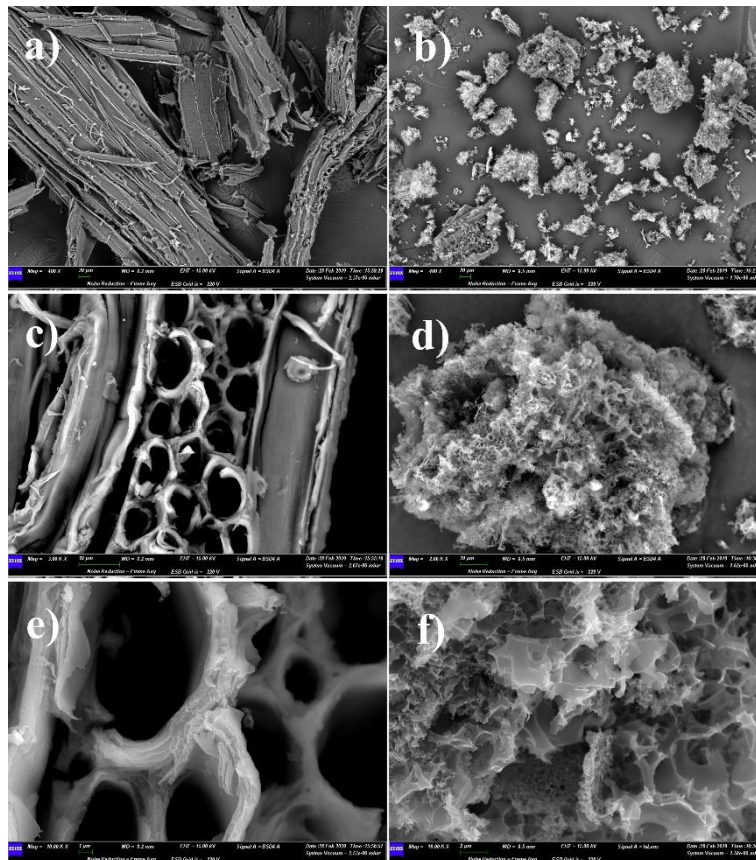**Figure 2.** Scanning electron microscopy (SEM) images of HC_200_0 (left-hand side: (**a**,**c**,**d**) and HCA_200_0 (right-hand side: (**b**), (**d**,**f**) at different magnification: (**a**,**b**) 400×; (**c**) 3000×; (**d**) 2000×; (**e**,**f**) 10,000×.

The EDS analysis, not reported here, shows the carbon as the main element with a distributed trace of chlorine, owing to the HCl washing step of the activation method.

As far as the time course of the outflowing CO_2 and CH_4 concentration is concerned, a sigmoidal behavior was observed for all tests and at all values of the operating pressure, as shown in Figure 3. The recorded signals are reported as a normalized value, that is, divided by the inlet concentration.
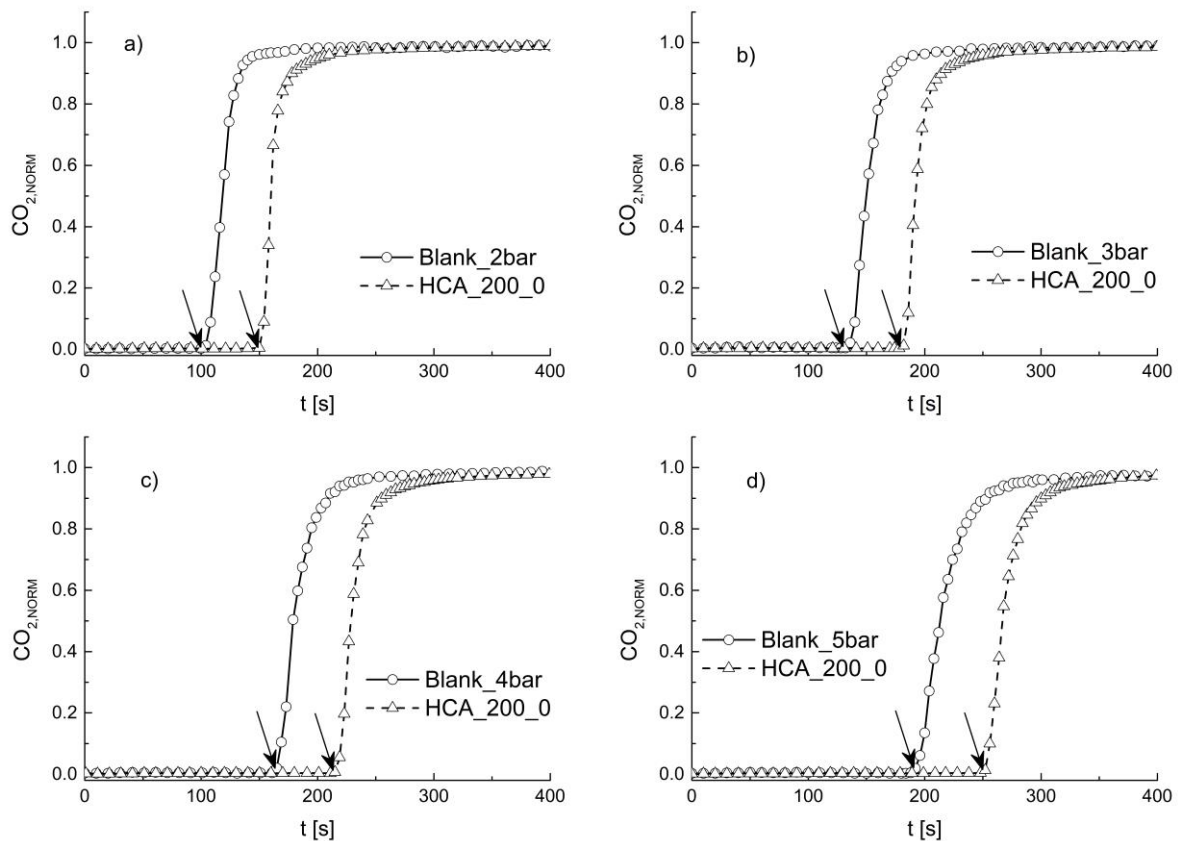

Figure 3. CO_2/N_2 adsorption curves at (**a**) 2 bar; (**b**) 3 bar; (**c**) 4 bar; and (**d**) 5 bar.

By inspection of Figure 3, the time of first detection (arrows) depends evidently on the operating pressure. The translation of blank curves is inherent in the operating modality of the apparatus and depends linearly on the pressure (data not reported for the sake of brevity). The translation of the response curves suffers from the superimposition owing to the presence of the adsorbent bed. The difference between the two delays increases steadily. Table 3 is a synopsis of all the results.

The sorbent capacity of the activated hydrochar obtained at 200 °C and 0 min is higher than that of the corresponding material recovered after 120 min of retention in the HTC reactor. The results of the BET analysis confirm this finding, where the 0 minute sample shows a specific area as high as 210% (3.1 time bigger) and an average pore diameter decreased by 27% in comparison with sample HCA_200_120. These results warn that the HTC reaction time is a crucial parameter and that the existence of a possible optimal retention time will be worth study, and in the further developments, it will be coupled with a cost optimization aimed at industrial exploitation of the results.

On the other hand, the performances of non-activated hydrochar denounce of an adsorbent capacity of an order of magnitude lower, and are thus not acceptable for industrial applications.

Table 3. CO_2 sorbent capacity.

Sample	TEST	P [bar]	Sorbent Capacity * [mmol/g]
HC_200_120	CO_2/N_2	2	0.335 ± 0.129
		3	0.425 ± 0.181
		4	0.688 ± 0.210
		5	0.692 ± 0.228
HCA_200_120	CO_2/N_2	2	2.651 ± 0.225
		3	3.366 ± 0.292
		4	3.475 ± 0.368
		5	3.635 ± 0.268
HCA_200_0	CO_2/N_2	2	4.957 ± 0.952
		3	5.658 ± 0.070
		4	6.199 ± 0.081
		5	6.569 ± 0.119

* Mean ± standard deviation.

Figure 4 shows typical adsorption curves obtained with the activated hydrochar at 2 and 5 bar (a and b, respectively) and the mixture CH_4/CO_2. Blank runs are reported as a reference. Arrows signal the time of the first detection. Both diagrams show that, in the blank runs, the CO_2 and CH_4 signals are indistinguishable. On the contrary, in the presence of a hydrochar bed, a selectivity appears evident, as proven by the temporal separation of the arrows. Methane appears first in the column outlet regardless of the operating pressure. The delay between the two signals is an increasing function of the operating pressure, and in any case, it is sufficiently broad for envisaging the development of an industrial process. All of this evidence proves that hydrochar is a suitable medium for separating the mixture by selective adsorption.
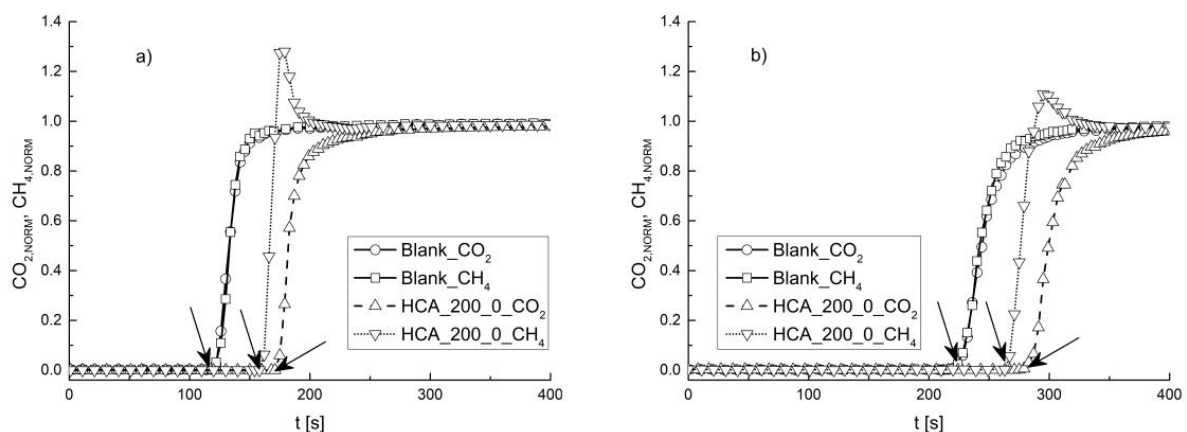

**Figure 4.** CO_2/CH_4 adsorption curves at (**a**) 2 bar and (**b**) 5 bar.

Table 4 quotes the obtained selectivities and recoveries calculated using Equations (1)–(3). The obtained selectivities confirm that CO_2 is preferred to CH_4. The performance of hydrochar is worse than that obtainable with commercial porous sorbents such as zeolites or activated carbons [22]. As expected, the methane recovery is relatively low with a purity of 95% (Italian regulation for network injection) regardless of the investigated operating pressure. The doubling of recovery obtained with a purity of 70% is a valuable result because of energetic applications.

Table 4. Summary of the results of the adsorption tests (mixture CO_2/CH_4).

Sample	TEST	P [bar]	Recovery (Purity = 95%) [%]	Recovery (Purity = 70%) [%]	Selectivity
HCA_200_0	CO_2/CH_4	2	31.98 ± 0.13	60.12 ± 0.35	1.88 ± 0.02
		5	36.09 ± 0.87	68.11 ± 0.10	2.10 ± 0.02

Figure 5 reports the averaged CO_2 sorbent capacity for the two samples of activated hydrochar as a function of the corresponding partial pressure in the gas phase. Data fit well to the Langmuir equation [47].

$$CO_{2\text{Sorbent capacity}} = \left(C_{\text{Max}} \cdot p_{CO_2}\right) / \left(K + p_{CO_2}\right) \tag{4}$$
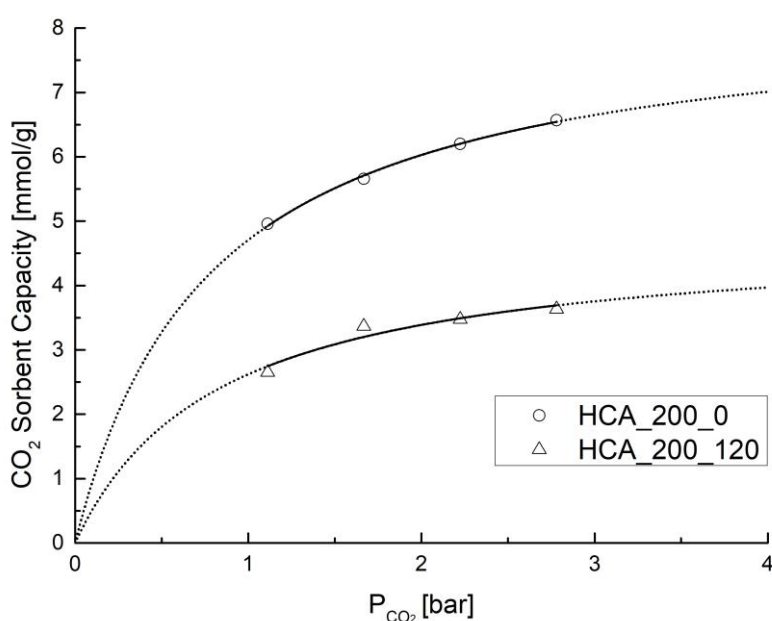
Figure 5. CO_2 sorbent capacity vs. p_{CO2}.

The regressions are reported as solid lines in the explored range and as dotted lines in the extrapolated ones. A wider partial pressure range should be explored to ascertain the correct equilibrium law. For the present paper, this preliminary investigation gives valuable information for steering future studies.

The regression parameters are reported in Table 5.

Table 5. Synopsis of regression parameters for Langmuir equation.

	C_{Max}	K	R^2
HCA_200_0	8.38 ± 0.15	0.77 ± 0.05	0.99
HCA_200_120	4.79 ± 0.45	0.83 ± 0.26	0.90

Figures 6 and 7 compare the performances of the hydrochars to those of traditional solid materials and those of some innovative materials, as reported in the literature [22,40,48–54]. As a general finding, data on PSA at 1 bar appear in the literature sparingly, even for traditional sorption media. Figure 6 reports a possible comparison of the hydrochar sorption capacity. It appears that, despite the different capture techniques, the data of "HCA_200_0_calc" at 1 bar (calculated by Equation (4)) are comparable with those of the literature. On the other hand, the comparison with PSA experiments conducted on

zeolites, activated carbon, and fly ash shows that, at the same operating conditions, the HCA exhibits much better results in terms of CO_2 capture capacity.
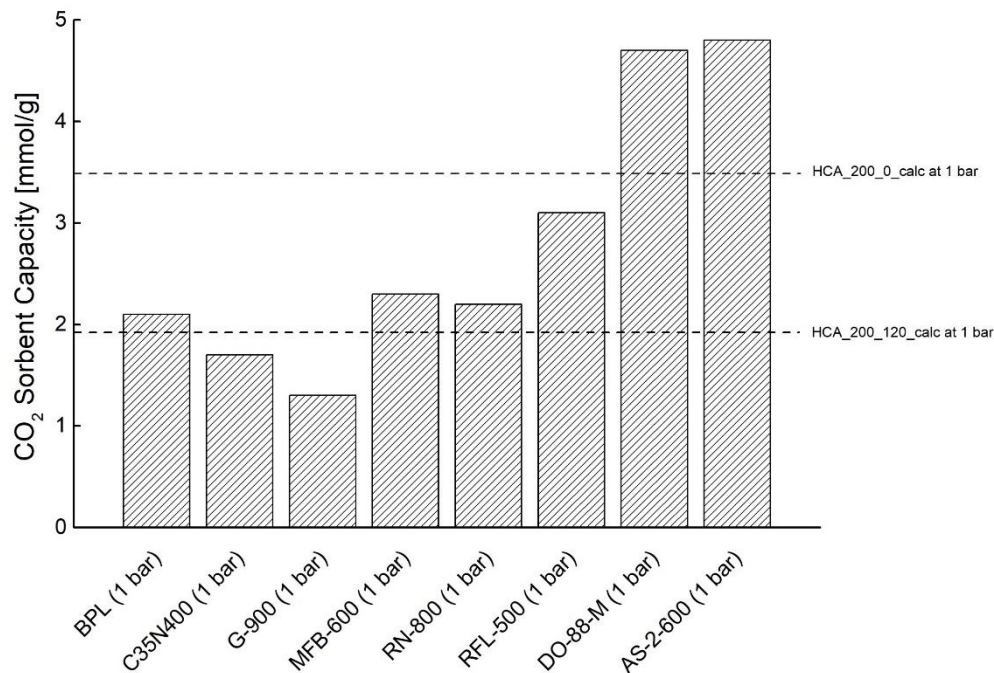
Figure 6. Comparison of CO_2 sorbent capacities with literature data obtained with batch equilibrium method (BPL: commercial activated carbon [48]; C35N400: ammonia-treated activated carbon [49]; G-900: activated graphite fibers [50]; MFB-600: N-doped activated carbon [51]; RN-800: ammonia-treated activated carbon [52]; RFL-500: N-doped porous carbon [53]; DO-88-M: activated carbon from petroleum pitch [54]; AS-2-600: sawdust-based porous carbon [40]).
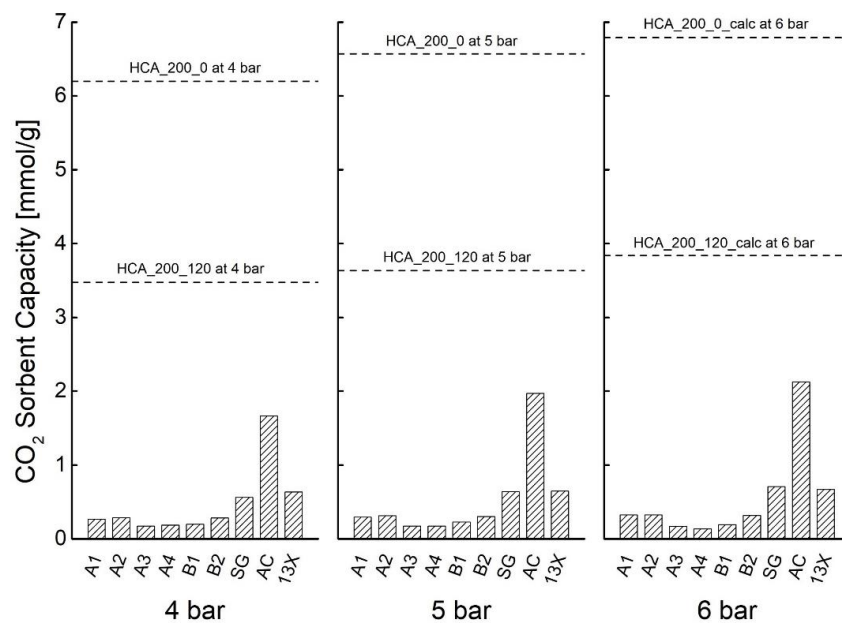
Figure 7. Comparison of CO_2 sorbent capacities with literature data obtained with the dynamic experimental method (pressure swing adsorption (PSA)) (A1, A2, A3, A4, B1, B2: zeolites from fly ash; SG: commercial silica gel; AC: commercial activated carbon; 13X: commercial zeolite [22]).

Figure 7 shows that the HCA_200_0 has the best CO_2 sorbent capacity: 6.569 mmol/g, threefold concerning the best performance of traditional sorbents [22]. Another significant result appears in Figure 7. Hydrochars prepared after 120 min of HTC reaction halve their performance, even though remaining well above commercial zeolites and similar materials. This suggests investing in further research aimed to ascertain if a reaction time exists, which maximizes the sorption capacity. This more-in-depth investigation is of the utmost importance for industrial-scale process optimization.

All of the results here reported highlight the concrete possibility of exploiting the residual biomass as an adsorption medium for biogas upgrading and encourages continuing research in this way.

4. Conclusions

Hydrochar from lignocellulosic residual biomass furnishes porous carbon materials via usual activation. The best reaction conditions were 200 °C and 0 min. The best results were BET area of 881 m^2/g, average pore diameter of 11 Å, and sorbent capacity of 6.569 mmol/g at 5 bar. The hydrochar exhibits higher CO_2 adsorption than that of some traditional sorbents. The material possesses adequate capacity to adsorb CO_2 from mixtures with CH_4 selectively. This residual material could be exploited in a sustainable biogas upgrading process, contextually reducing CO_2 emissions and the related environmental impact.

References

1. Vitillo, J.G.; Smit, B.; Gagliardi, L. Introduction: Carbon Capture and Separation. *Energy Convers. Manag.* **2002**, *43*, 63–75. [CrossRef]

2. IEA International Energy Agency (Paris (France)). *Technology Roadmap: Carbon Capture and Storage*. 2013. Available online: https://insideclimatenews.org/sites/default/files/IEA-CCS%20Roadmap.pdf (accessed on 8 March 2020).

3. NOAA National Centers for Environmental Information. State of the Climate: Global Climate Report for September 2018. 2018. Available online: https://www.ncdc.noaa.gov/sotc/global/201809 (accessed on 8 March 2020).

4. Hoegh-Guldberg, O.; Jacob, D.; Taylor, M.; Bindi, M.; Brown, S.; Camilloni, I.; Diedhiou, A.; Djalante, R.; Ebi, K.L.; Engelbrecht, F.; et al. Impacts of 1.5 °C Global Warming on Natural and Human Systems. In *Global Warming of 1.5 °C. An IPCC Special Report on the Impacts of Global Warming of 1.5 °C above Pre-Industrial Levels and Related Global Greenhouse Gas Emission Pathways, in the Context of Strengthening the Global Response to the Threat of Climate Change, Sustainable Development, and Efforts to Eradicate Poverty*; IPCC Secretariat: Geneva, Switzerland, 2018.

5. IPCC. Annex II: Glossary. In *Climate Change 2014: Synthesis Report. Contribution of Working Groups I, II and III to the Fifth Assessment Report of the Intergovernmental Panel on Climate Change*; Core Writing Team, Pachauri, R.K., Meyer, L.A., Eds.; IPCC: Geneva, Switzerland, 2014; pp. 117–130.

6. WHO. *COP24 Special Report: Health and Climate Change*; World Health Organization: Geneva, Switzerland, 2018; Available online: http://apps.who.int/iris (accessed on 9 March 2020).

7. European Commission. 2030 Climate & Energy Framework. 2014. Available online: https://ec.europa.eu/clima/policies/strategies/2030_en (accessed on 8 March 2020).

8. European Commission. Paris Agreement 2015. Available online: https://ec.europa.eu/clima/policies/international/negotiations/paris_en (accessed on 8 March 2020).

9. Harrison, D.P. Sorption-Enhanced Hydrogen Production: A Review. *Ind. Eng. Chem. Res.* **2008**, *47*, 6486–6501. [CrossRef]

10. Jain, S.; Jain, S.; Wolf, I.T.; Lee, J.; Tong, Y.W. A comprehensive review on operating parameters and different pretreatment methodologies for anaerobic digestion of municipal solid waste. *Renew. Sustain. Energy Rev.* **2015**, *52*, 142–154. [CrossRef]

11. Ryckebosch, E.; Drouillon, M.; Vervaeren, H. Techniques for transformation of biogas to biomethane. *Biomass Bioenergy* **2011**, *35*, 1633–1645. [CrossRef]

12. EBA—European Biomass Association. EBA Biomethane & Biogas Report 2015. 2015. Available online: http://european-biogas.eu/2015/12/16/biogasreport2015/ (accessed on 8 March 2020).

13. Favre, E. Carbon dioxide recovery from post-combustion processes: Can gas permeation membranes compete with absorption? *J. Memb. Sci.* **2007**, *294*, 50–59. [CrossRef]

14. Khan, I.U.; Othman, M.H.D.; Hashim, H.; Matsuura, T.; Ismail, A.F.; Rezaei-DashtArzhandi, M.; Azelee, I.W. Biogas as a renewable energy fuel—A review of biogas upgrading, utilisation and storage. *Energy Convers. Manag.* **2017**, *150*, 277–294. [CrossRef]

15. Tuinier, M.J.; van Sint Annaland, M.; Kramer, G.J.; Kuipers, J.A.M. Cryogenic CO_2 capture using dynamically operated packed beds. *Chem. Eng. Sci.* **2010**, *65*, 114–119. [CrossRef]

16. Olajire, A.A. CO_2 capture and separation technologies for end-of-pipe applications—A review. *Energy* **2010**, *35*, 2610–2628. [CrossRef]

17. Mondal, M.K.; Balsora, H.K.; Varshney, P. Progress and trends in CO_2 capture/separation technologies: A review. *Energy* **2012**, *46*, 431–441. [CrossRef]

18. Haefeli, S.; Bosi, M.; Philibert, C. Carbon Dioxide Capture and Storage Issues. Accounting and Baselines under the United Nations Framework Convention on Climate Change (UNFCCC). IEA Information Paper. Available online: https://www.osti.gov/etdeweb/biblio/20543208 (accessed on 8 March 2020).

19. Quintella, C.M.; Hatimondi, S.A.; Musse, A.P.S.; Miyazaki, S.F.; Cerqueira, G.S.; De Araujo Moreira, A. CO_2 capture technologies: An overview with technology assessment based on patents and articles. *Energy Procedia* **2011**, *4*, 2050–2057. [CrossRef]

20. Zhao, Z.; Cui, X.; Ma, J.; Li, R. Adsorption of carbon dioxide on alkali-modified zeolite 13X adsorbents. *Int. J. Greenh. Gas. Control* **2007**, *1*, 355–359. [CrossRef]

21. Liu, Y.; Lin, X.; Wu, X.; Liu, M.; Shi, R.; Yu, X. Pentaethylenehexamine loaded SBA-16 for CO_2 capture from simulated flue gas. *Powder Technol.* **2017**, *318*, 186–192. [CrossRef]

22. Ferella, F.; Puca, A.; Taglieri, G.; Rossi, L.; Gallucci, K. Separation of carbon dioxide for biogas upgrading to biomethane. *J. Clean. Prod.* **2017**, *164*, 1205–1218. [CrossRef]

23. Dawson, R.; Cooper, A.I.; Adams, D.J. Chemical functionalization strategies for carbon dioxide capture in microporous organic polymers. *Polym. Int.* **2013**, *62*, 345–352. [CrossRef]

24. Kenarsari, S.D.; Yang, D.; Jiang, G.; Zhang, S.; Wang, J.; Russell, A.G.; Weif, Q.; Fan, M. Review of recent advances in carbon dioxide separation and capture. *RSC Adv.* **2013**, *3*, 22739–22773. [CrossRef]

25. Philibert, C. Technology Penetration and Capital Stock Turnover. Lessons from IEA Scenario Analysis. France. 2007. Available online: http://www.oecd.org/dataoecd/55/52/38523883.pdf (accessed on 8 March 2020).

26. Chakravarti, S.; Gupta, A.; Hunek, B. Advanced Technology for the Capture of Carbon Dioxide from Flue Gases. In Proceedings of the First National Conference on Carbon Sequestration, Washington, DC, USA, 14–17 May 2001; U.S. Department of Energy National Energy Technology Laboratory: Washington, DC, USA, 2001; pp. 1–11. [CrossRef]

27. IPCC. *Carbon Dioxide Capture and Storage*; Metz, B., Davidson, O., de Coninck, H., Loos, M., Meyer, L., Eds.; Cambridge University Press: New York, NY, USA, 2005; 431p, Available online: https://archive.ipcc.ch/pdf/special-reports/srccs/srccs_wholereport.pdf (accessed on 8 March 2020).

28. Wang, M.; Lawal, A.; Stephenson, P.; Sidders, J.; Ramshaw, C. Post-combustion CO_2 capture with chemical absorption: A state-of-the-art review. *Chem. Eng. Res. Des.* **2011**, *89*, 1609–1624. [CrossRef]

29. Titirici, M.M.; White, R.J.; Falco, C.; Sevilla, M. Black perspectives for a green future: Hydrothermal carbons for environment protection and energy storage. *Energy Environ. Sci.* **2012**, *5*, 6796–6822. [CrossRef]

30. Berge, N.D.; Ro, K.S.; Mao, J.; Flora, J.R.V.; Chappell, M.A.; Bae, S. Hydrothermal carbonization of municipal waste streams. *Environ Sci. Technol.* **2011**, *45*, 5696–5703. [CrossRef]

31. Uddin, H.M.; Reza, M.T.; Lynam, J.G.; Coronella, J.C. Effects of Water Recycling in Hydrothermal Carbonization of Loblolly Pine. *Environ. Prog. Sustain.* **2013**, *33*, 1309–1315. [CrossRef]

32. Stemann, J.; Ziegler, F. Hydrothermal Carbonisation (Htc): Recycling of Process Water. In Proceedings of the 19th European Biomass Conferences and Exhibition, Berlin, Germany, 6–10 June 2011.

33. Gallifuoco, A.; Taglieri, L.; Scimia, F.; Papa, A.A.A.; Di Giacomo, G. Hydrothermal carbonization of Biomass: New experimental procedures for improving the industrial Processes. *Bioresour Technol.* **2017**, *244*, 160–165. [CrossRef]

34. Gallieri, A.; Taglieri, L.; Papa, A.A.; Scimia, F.; Di Giacomo, G. Hydrothermal conversions of waste biomass: Assessment of kinetic models using liquid-phase electrical conductivity measurements. *Waste Manag.* **2018**, *77*, 586–592. [CrossRef] [PubMed]

35. Mariscal, R.; Maireles-Torres, P.; Ojeda, M.; Sádaba, I.; López Granados, M. Furfural: A renewable and versatile platform molecule for the synthesis of chemicals and fuels. *Energy Environ. Sci.* **2016**, *9*, 1144–1189. [CrossRef]

36. Centi, G.; Lanzafame, P.; Perathoner, S. Analysis of the alternative routes in the catalytic transformation of lignocellulosic materials. *Catal. Today* **2011**, *167*, 14–30. [CrossRef]

37. Reza, M.T.; Andert, J.; Wirth, B.; Busch, D.; Pielert, J.; Lynam, J.G.; Mumme, J. Hydrothermal Carbonization of Biomass for Energy and Crop Production. *Appl. Bioenergy* **2014**, *1*, 11–29. [CrossRef]

38. Kruse, A.; Funke, A.; Titirici, M.M. Hydrothermal conversion of biomass to fuels and energetic materials. *Curr. Opin. Chem. Biol.* **2013**, *17*, 515–521. [CrossRef] [PubMed]

39. Román, S.; Valente Nabais, J.M.; Ledesma, B.; González, J.F.; Laginhas, C.; Titirici, M.M. Production of low-cost adsorbents with tunable surface chemistry by conjunction of hydrothermal carbonization and activation processes. *Microporous Mesoporous Mater.* **2013**, *165*, 127–133. [CrossRef]

40. Sevilla, M.; Fuertes, A.B. Sustainable porous carbons with a superior performance for CO_2 capture. *Energy Environ. Sci.* **2011**, *4*, 1765–1771. [CrossRef]

41. Farjon, A. *Abies alba*. The IUCN Red List of Threatened Species 2017: E.T42270A83978869. Available online: https://www.iucnredlist.org/species/42270/83978869 (accessed on 2 March 2020).

42. Brunauer, S.; Emmett, P.H.; Teller, E. Adsorption of Gases in Multimolecular Layers. *J. Am. Chem. Soc.* **1938**, *60*, 309–319. [CrossRef]

43. Barrett, E.P.; Joyner, L.G.; Halenda, P.P. The Determination of Pore Volume and Area Distributions in Porous Substances. I. Computations from Nitrogen Isotherms. *J. Am. Chem. Soc.* **1951**, *73*, 373–380. [CrossRef]

44. Thommes, M.; Kaneko, K.; Neimark, A.V.; Olivier, J.P.; Rodriguez-Reinoso, F.; Rouquerol, J.; Sing, K.S.W. Physisorption of gases, with special reference to the evaluation of surface area and pore size distribution (IUPAC Technical Report). *Pure Appl. Chem.* **2015**, *87*, 1051–1069. [CrossRef]

45. Di Felice, L.; Foscolo, P.; Gibilaro, L.G. CO_2 capture by dolomite particles in a gas fluidized bed: Experimental Data and Numerical Simulations. *Int. J. Chem. React. Eng.* **2011**, *9*, 1542–6580. [CrossRef]

46. Ruayruay, W.; Khongtong, S. Impregnation of Natural Rubber into Rubber Wood: A Green Wood Composite. *BioResources* **2014**, *9*. [CrossRef]

47. Rackley, S.A. 7-Adsorption capture systems. In *Carbon Capture and Storage*, 2nd ed.; Rackley, S.A., Ed.; Butterworth-Heinemann: Oxford, UK, 2017; ISBN 9780128120415. [CrossRef]

48. Kikkinides, E.S.; Yang, R.T.; Cho, S.H. Concentration and recovery of carbon dioxide from flue gas by pressure swing adsorption. *Ind. Eng. Chem. Res.* **1993**, *32*, 2714–2720. [CrossRef]

49. Przepiórski, J.; Skrodzewicz, M.; Morawski, A. High temperature ammonia treatment of activated carbon for enhancement of CO_2 adsorption. *Appl. Surf. Sci.* **2004**, *225*, 235–242. [CrossRef]

50. Meng, L.-Y.; Park, S.-J. Effect of heat treatment on CO_2 adsorption of KOH-activated graphite nanofibers. *J. Colloid Interface Sci.* **2010**, *352*, 498–503. [CrossRef]

51. Pevida, C.; Drage, T.C.; Snape, C.E. Silica-templated melamine–formaldehyde resin derived adsorbents for CO_2 capture. *Carbon* **2008**, *46*, 1464–1474. [CrossRef]

52. Plaza, M.G.; Pevida, C.; Arias, B.; Fermoso, J.; Rubiera, F.; Pis, J.J. A comparison of two methods for producing CO_2 capture adsorbents. *Energy Procedia* **2009**, *1*, 1107–1113. [CrossRef]

53. Hao, G.-P.; Li, W.-C.; Qian, D.; Lu, A.-H. Rapid Synthesis of Nitrogen-Doped Porous Carbon Monolith for CO_2 Capture. *Adv. Mater.* **2010**, *22*, 853–857. [CrossRef]

54. Wahby, A.; Ramos-Fernández, J.M.; Martínez-Escandell, M.; Sepúlveda-Escribano, A.; Silvestre-Albero, J.; Rodríguez-Reinoso, F. High-Surface-Area Carbon Molecular Sieves for Selective CO_2 Adsorption. *ChemSusChem* **2010**, *3*, 974–981. [CrossRef]